New Insights on Gas Hydroquinone Clathrates Using in Situ Raman Spectroscopy: Formation/Dissociation Mechanisms, Kinetics, and Capture Selectivity

R. Coupan, Eve Péré, Christophe Dicharry, Jean-Philippe Torre

New Insights on Gas Hydroquinone Clathrates Using in Situ Raman Spectroscopy: Formation/Dissociation Mechanisms, Kinetics, and Capture Selectivity

Romuald Coupan,[†] Eve Péré,[‡] Christophe Dicharry,[†] and Jean-Philippe Torré*[,†]

[†]Laboratoire des Fluides complexes et leurs Réservoirs, CNRS/TOTAL/UNIV PAU & PAYS ADOUR, IPRA, UMR5150, 64000 Pau, France

[‡]Institut des Sciences Analytiques et de Physico Chimie pour l'Environnement et les Matériaux, Hélioparc, UNIV PAU & PAYS ADOUR, CNRS−UMR 5254−IPREM, Avenue du Président Pierre Angot, Pau F 64000, France

ABSTRACT: Hydroquinone (HQ) is known to form organic clathrates with different gaseous species over a wide range of pressures and temperatures. However, the enclathration reaction involving HQ is not fully understood. This work offers new elements of understanding HQ clathrate formation and dissociation mechanisms. The kinetics and selectivity of the enclathration reaction were also investigated. The focus was placed on HQ clathrates formed with CO_2 and CH_4 as guest molecules for potential use in practical applications for the separation of a CO_2/CH_4 gas mixture. The structural transition from the native form (α HQ) to the clathrate form (β HQ), as well as the reverse process, were tracked using in situ Raman spectroscopy. The clathrate formation was conducted at 323 K and 3.0 MPa, and the dissociation was conducted at 343 K and 1.0 kPa. The experiments with CH_4 confirmed that a small amount of gas can fill the α HQ before the phase transition from α to β HQ begins. The dissociation of the CO_2−HQ clathrates highlighted the presence of a clathrate structure with no guest molecules. We can therefore conclude that HQ clathrate formation and dissociation are two step reactions that pass through two distinct reaction intermediates: guest loaded α HQ and guest free β HQ. When an equimolar CO_2/CH_4 gas mixture is put in contact with either the α HQ or the guest free β HQ, the CO_2 is preferentially captured. Moreover, the guest free β HQ can retain the CO_2 quicker and more selectively.

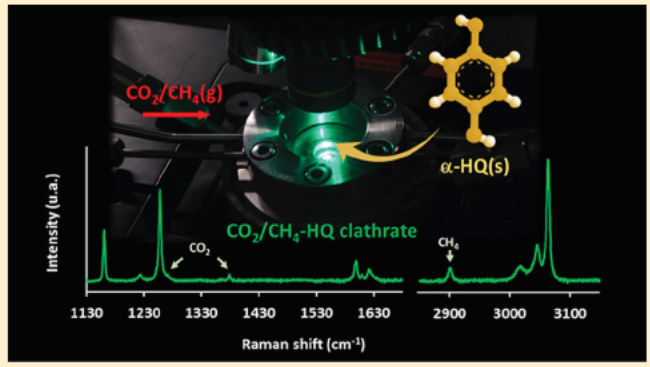

INTRODUCTION

Hydroquinone (HQ) is known to form gas clathrates, which are inclusion compounds consisting of a tridimensional network of self associating "host" molecules (in this case HQ) forming cavities capable of enclosing "guest" molecules of gas.[1] HQ has different polymorphisms: (i) the α form is its stable form at ambient pressure and temperature conditions,[2] (ii) the β form is its clathrate form,[3] (iii) the γ form is a metastable form prepared by sublimation from an HQ solution in ether,[4] and (iv) the δ form is amorphous.[5] α HQ has cavities at ambient conditions that are able to accommodate small gas molecules such as CO_2, SO_2, Ar, N_2, and H_2 with a ratio of 18:1 (i.e., 18 molecules of HQ per gas molecule).[2,3,6−10] Crystal structures obtained from X ray diffraction experiments, illustrating the exact position of the gas in α HQ, can be given as direct experimental evidence.[9,10] Note that gas inclusion in the α HQ cavities is not an enclathration phenomenon but rather a solubilization of gas molecules in the α phase, as these empty cavities are already present in the native structure of α HQ.[3,11−14] HQ gas clathrates (β HQ) are formed only in the presence of guest molecules (such as CO_2, CH_4, and N_2) at well defined conditions of pressure and temperature.[15] Generally speaking, HQ clathrates form with a maximum HQ/guest molar ratio of 3:1 (i.e., three molecules of HQ per guest molecule) with only one guest molecule per cavity, except in the particular case of H_2, for which several guest molecules have been found in the same HQ cavity at very high pressure.[16] HQ clathrates are thus characterized by an occupancy factor—that is, the proportion of cavities filled by guest molecules—of 0 to 1. It is worth noting that molecular crystals composed only of a network of empty cavities (i.e., no guest molecules) have been observed in certain conditions. As they derive from clathrate structures, they are called "guest free clathrates". Guest free HQ clathrates can be formed by recrystallization from an HQ solution in alcohol[17,18] or by a guest released from HQ clathrates (such as CO_2 and Xe HQ clathrates) as the temperature increases.[19−21] Such a "guest free" structure was also obtained recently from gas hydrates.[22]

It has also been highlighted that HQ clathrates can selectively capture CO_2 from various CO_2 containing gas mixtures (i.e.,

CO_2/CH_4, CO_2/N_2, and CO_2/H_2).[19,23−25] However, despite the high capture selectivity (i.e., 29 mol^{CO2}/mol^{CH4}) reported for equimolar CO_2/CH_4 mixtures,[19] this phenomenon cannot be explained by thermodynamic considerations based on the equilibrium curves of CO_2−HQ and CH_4−HQ clathrates (i.e., equilibrium curves very close to each other).[26] Consequently, to further develop CO_2 separation processes based on the use of HQ clathrates, a better understanding of their formation and dissociation mechanisms is crucial.

This work investigates the formation and dissociation of CO_2− and CH_4−HQ clathrates using in situ Raman spectros copy and studies both the mechanisms and kinetic aspects. In situ Raman spectroscopy is ideal for studying these clathrate compounds, which are, by nature, metastable outside of their thermodynamic stability conditions. In a controlled temper ature and pressure environment, this nonintrusive technique makes it possible to unambiguously differentiate α and β HQ structures. Accordingly, the Raman signatures of these two HQ polymorphisms are well known in literature and are easy to discriminate.[27−30] By means of in situ Raman spectroscopy tracking, Park et al. highlighted the temperature dependence of CO_2− and CH_4−HQ clathrate dissociation (i.e., the release of guest molecules and structural transition of clathrates),[30] and Lee et al. studied the kinetics of CO_2 uptake and release by HQ clathrates as a function of temperature.[19]

Furthermore, additional experiments were performed using an equimolar CO_2/CH_4 gas mixture in contact with either α HQ or guest free β HQ, in an attempt to better understand the selective enclathration phenomenon of HQ clathrates. A CO_2/CH_4 gas mixture was chosen for this study, as the separation of CO_2 from this mixture is a direct industrial case study for gas sweetening applications (i.e., removal of CO_2 and H_2S from production gas containing mainly CH_4). In applications such as these, the raw gas coming from the reservoir is already hot and pressurized (several MPa). As HQ clathrates can form in this type of condition, it could be very advantageous to separate the CO_2 from the mixture using HQ clathrate based processes. To be in line with conventional separation processes using gas−solid contactors (e.g., fixed or fluidized bed reactors), this study was performed using solid HQ (without any solvent) at two set operating points, realistic for these kinds of CO_2/CH_4 separation units: 323 K and 3.0 MPa for the clathrate formation and 343 K at 1.0 kPa for the dissociation. These operating conditions were also set based on the three phase equilibrium curve determined by Coupan et al. for CO_2− and CH_4−HQ systems[26] and are in line with the target application of gas sweetening.[31]

EXPERIMENTAL SECTION

Materials. HQ is provided by Acros Organics (purity of 99.5 mol %). For the experiments, the HQ is ground to obtain crystals with a mean particle size of ∼100 μm to promote the gas phase reaction. CO_2, CH_4, and a CO_2/CH_4 equimolar gas mixture (minimum mole fraction purity of 99.995%) are purchased from Linde Gas SA. The CO_2 mole fraction of the CO_2/CH_4 mixture is 50.1 ± 1.0% (analytical value given by the supplier).

Apparatus and Method. The spectroscopic experimental setup is detailed in Figure 1. Its main components are a high pressure measurement cell and a confocal microscope coupled to a Raman spectrometer. The customized high pressure cell (designed by Top Industrie, France) is made of TA6 V titanium and has a volume of 0.39 cm^3. It is fitted with a sapphire optical

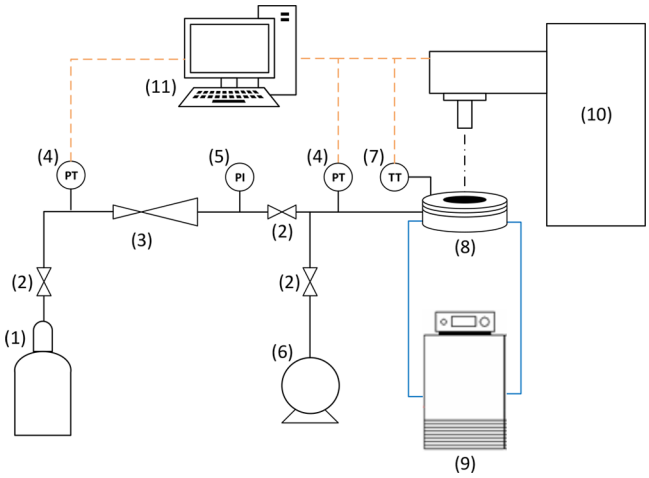

Figure 1. Experimental setup. (1) Gas tank; (2) plug valves; (3) gas expander; (4) pressure transmitters; (5) digital manometer; (6) vacuum pump; (7) temperature sensor; (8) Raman cell; (9) thermostatic bath; (10) Raman spectrometer; (11) visualization and acquisition system.

window of 33 mm in diameter and 3.5 mm thick allowing in situ Raman spectroscopy experiments to be run at pressures and temperatures of up to 20 MPa and 423 K, respectively. The cell is connected to a gas storage tank and a vacuum pump. The temperature in the cell is maintained at the required value by continuous forced circulation of silicone oil through the cell jacket by means of a thermostatic bath (Polystat 37, Fischer Scientific). The cell is firmly held to prevent any vibrations due to circulation of the liquid. Temperature is measured by a thermocouple (accuracy of ±0.2 K) located directly in the cell. Pressure is measured by a digital manometer (model Leo II from Keller with an uncertainty of ±0.01 MPa) and a 0−10 MPa pressure transmitters (model PA33X from Keller with an uncertainty of ±0.01 MPa) both located on the gas inlet line. The Raman spectrometer (T64000 Jobin Yvon) works with a Raman notch filter that helps eliminate Rayleigh scattering and uses 1800 grooves/mm grating, allowing a spectral resolution of 2 cm^{-1}. The excitation source is the 514.5 nm line of an argon ion laser. The analysis is performed in the 3300−300 cm^{-1} region with an acquisition time of 60 s. With a confocal aperture of 200 μm and a 10× magnification objective lens, a surface area of 25 μm^2 and a depth of 2 μm can be analyzed. These parameters (confocal aperture and magnification) were chosen for the following reasons: (i) so that we would not have to consider the entire spectral response of the gas, (ii) to maximize the volume analyzed, and (iii) to prevent intensity loss when passing through the sapphire window and the gas phase. The laser beam is focused on the crystal surface by means of a camera (from JVC) allowing visualization of the sample. The Raman shift wavenumber calibration (i.e., calibration of the detector) is initially performed by reference to the silicon band at 520 cm^{-1}. The calibration is then checked, before each measurement, against the sapphire band (of the cell) at 417 cm^{-1} to avoid variations due to room temperature change or mechanical drift.

Owing to this experimental setup, tracking of the spectral signature as a function of time is conducted under controlled pressure and temperature conditions. For the experiments, ∼0.1 g of powdered HQ is loaded into the cell. To check the experimental repeatability and homogeneity of the measure

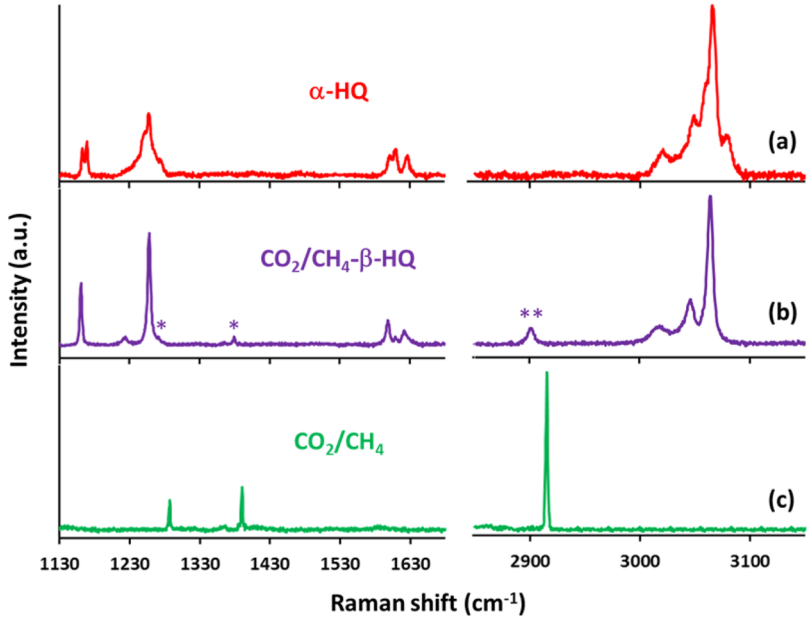

Figure 2. Raman spectra of (a) the α HQ, (b) the CO_2/CH_4–HQ clathrates, and (c) the equimolar CO_2/CH_4 gas mixture, for Raman shifts ranging from 1130 to 1680 cm^{-1} and 2850 to 3150 cm^{-1}. The single asterisks show the Raman bands of CO_2 guest molecules at 1272 and 1380 cm^{-1} and the double asterisk the CH_4 guest molecules at 2904 cm^{-1}. The intensities are given in arbitrary units (a.u.).

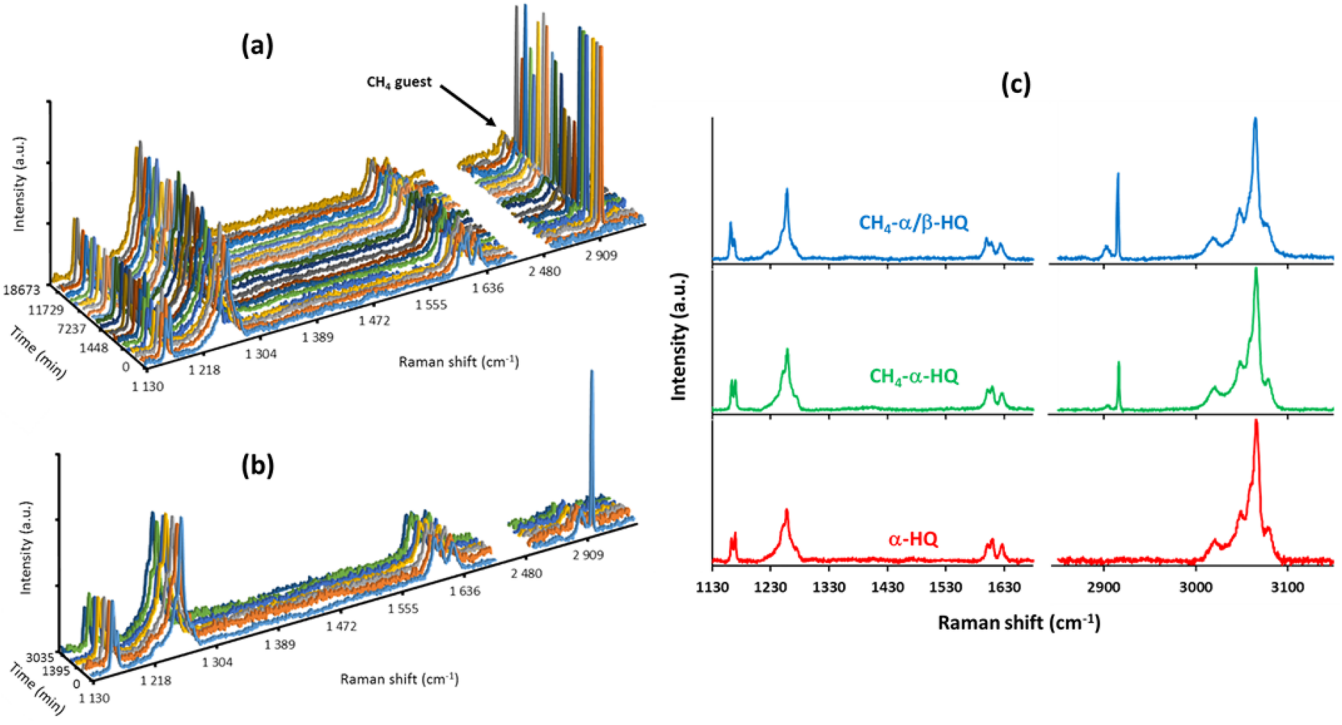

Figure 3. Raman spectroscopic tracking of (a) the formation, at 3.0 MPa and 323 K, and (b) the dissociation, at 1.0 kPa and 343 K, of CH_4–HQ clathrates. (c) Raman spectra of the α HQ, the CH_4 α HQ, and an ongoing transition form CH_4 α/β HQ. The intensities are given in arbitrary units (a.u.).

ments, a minimum of six crystals are analyzed throughout each experiment (the same crystals are tracked from the beginning to the end, and the data are averaged). The temperature is set at the required value, and the whole system (the Raman cell and the piping) is put under vacuum at 1 kPa. Next, the gas is loaded into the cell, and the gas pressure is kept constant at the target value. For the clathrate formation, the temperature and pressure conditions are 323 K and 3.0 MPa. The clathrate dissociation is performed by changing the previous conditions to 343 K and 1 kPa.

RESULTS AND DISCUSSION

Figure 2 presents the Raman spectra of the α HQ (Figure 2a) and the CO_2/CH_4–HQ clathrates (Figure 2b). Even though the same covalent bonds exist in both HQ forms, the two HQ structures can nevertheless be differentiated, as there are some

dissimilarities in their vibrational modes due to different molecular environments in their respective hydrogen bonded organic frameworks.

Results showed some differences between the α and β HQ spectra, the main ones being: (i) the two C−H bending bands at 1163 and 1169 cm^{-1} in the α HQ spectrum appeared as a single band at 1163 cm^{-1} in the clathrate spectrum; (ii) the coupled C−O and C−C stretching band shifted from 1257 cm^{-1} in the α HQ spectrum to 1260 cm^{-1} in the β HQ spectrum; (iii) there were changes in the relative intensities of the three C−C stretching bands at ∼1600 cm^{-1}; and (iv) the C−H stretching band at 3080 cm^{-1} in the α HQ spectrum was absent in the HQ clathrate spectra. In addition, slight changes in the relative intensities of the C−O bending and C−C stretching bands could also be detected at ∼480 and 850 cm^{-1} (this spectral zone is not shown in Figure 2). Moreover, Raman spectroscopy made it possible to clearly identify the presence of CO_2 and CH_4 guest molecules in the HQ clathrates. In the case of the CO_2 molecules, the symmetrical C═O stretching bands were observed at 1272 and 1380 cm^{-1},[29,32,33] and in the case of the CH_4 molecules, the symmetrical C−H stretching bands were at 2905 cm^{-1}.[34] It is worth noting that, based on the analysis of the equimolar CO_2/CH_4 mixture (Figure 2c), CO_2 could be detected at 1287 and 1390 cm^{-1} and CH_4 at 2915 cm^{-1}. The differences between the Raman spectroscopic signatures in the gas phase and in the clathrate phase for the CO_2 and the CH_4 were clearly noticeable and could be mainly ascribed to the presence of host−guest interactions and to the spatial constraints of the molecules trapped in clathrate lattices. Overall, the position of the bands in all the spectra shown in Figure 2 (i.e., the Raman shift) were in very good agreement with literature data.[27−29]

Formation and Dissociation of the CH_4−HQ Clathrates. Figure 3 shows the spectroscopic tracking as a function of time during the formation and dissociation of CH_4−HQ clathrates.

For the first 3000 min of the formation experiment (Figure 3a), there was no significant change in the spectral signature of the HQ molecules (i.e., the HQ Raman spectra indicated that the sample was α HQ). We observed the following: (i) the two C−H bending bands at 1163 and 1169 cm^{-1}, (ii) the coupled C−O and C−C stretching band at 1257 cm^{-1}, and (iii) the three C−C stretching bands at ∼1600 cm^{-1}, where the middle band was the most intense. Furthermore, no characteristic band of β HQ was detected. During this period, however, the C−H stretching band of encaged CH_4 molecules started to appear at 2904 cm^{-1}, and its intensity then slowly increased over time. This observation shows that the α HQ is first filled with CH_4 molecules, forming the intermediate guest loaded α HQ. The Raman spectrum of this intermediate is shown in Figure 3c. The CH_4 gas band was also detected at 2915 cm^{-1} during the formation step under pressure conditions. The Raman intensity of this gas band fluctuated over time according to the focus height. After this step, the Raman bands evolved continuously from the spectral signature of α HQ to that of β HQ. Indeed, the two C−H bending bands at 1163 and 1169 cm^{-1} progressed to form a single band at 1163 cm^{-1}, the coupled C−O and C−C stretching band shifted from 1257 to 1260 cm^{-1}, and the relative intensities of the three C−C stretching bands at 1598, 1609, and 1621 cm^{-1} varied over time. Moreover, the intensity of the Raman bands of the encaged CH_4 molecules progressively increased. At the end of the formation step, a small shoulder was detected on the C−H bending bands at 1163 cm^{-1} (see Figure 3c), revealing the presence of residual α HQ in the final product (i.e., the α to β conversion is not total). It is therefore possible to deduce that CH_4−HQ clathrate formation is a two step mechanism. Equations 1 and 2 presented below summarize this mechanism considering HQ/guest molar ratios of 18:1 for the first step and 3:1 for the second:

$$18HQ^{\alpha} + x^{\alpha}CH_4 \rightarrow x^{\alpha}CH_4 \cdot 18HQ^{\alpha} \quad (1)$$

$$x^{\alpha}CH_4 \cdot 18HQ^{\alpha} + (6x - x^{\alpha})CH_4 \rightarrow 6[xCH_4 \cdot 3HQ^{\beta}] \quad (2)$$

where x^{α} and x are the α HQ and the β HQ occupancies, respectively. In the actual case study, we were unable to affirm whether the CH_4 molecules filled the α HQ (i.e., $x^{\alpha} = 1$) entirely, or whether α HQ was simply filled to a critical occupancy before the transition from α to β HQ began.

Concerning the dissociation of the CH_4−HQ clathrates, Figure 3b shows a decrease in the intensity of the CH_4 band along with changes in the HQ bands from the β HQ to the α HQ signature. The two intermediates, CH_4 α HQ, and the guest free β HQ were not observed during the dissociation step. Additional dissociation experiments performed in milder conditions at 323 K (instead of 343 K) and 0.1 MPa (instead of 1.0 kPa) failed to show that guest free HQ clathrates could derive from CH_4−HQ clathrates.

To also investigate the kinetic aspects of these reactions, the ratio of the CH_4 band at 2904 cm^{-1} to the HQ band at 1259 cm^{-1} was represented as a function of time for the formation and dissociation of CH_4−HQ clathrates (Figure 4). The HQ band at 1259 cm^{-1} was chosen as the normalization reference due to its very slight modification over time. Normalization is necessary to overcome the intensity fluctuation of the signal due to the focus height. The accuracy of the method (error bars represented in the graphs) arises from both the averaging of the results obtained from the crystals and from the baseline fluctuations over time. The magnitude of the error bars principally reveals the high variability in the formation kinetics measured on each isolated crystal (i.e., the clathrate formation kinetics are very different from one crystal to another), making it impossible to determine reaction rates. The graph does however give qualitative information on the global kinetic trend. On the basis of the experiments, the induction period (i.e., the waiting period during which the α HQ starts to transform into β HQ) was estimated to be 60 ± 10 h, and the

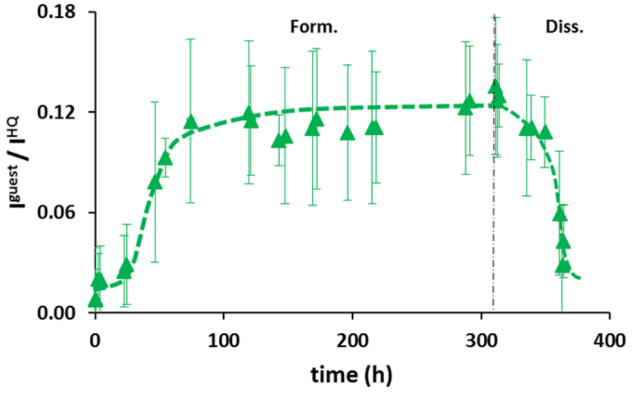

Figure 4. Formation at 3.0 MPa and 323 K and dissociation at 1.0 kPa and 343 K of CH_4−HQ clathrates. Ratio of the intensities of the CH_4 band at 2904 cm^{-1} to the HQ band at 1259 cm^{-1}.

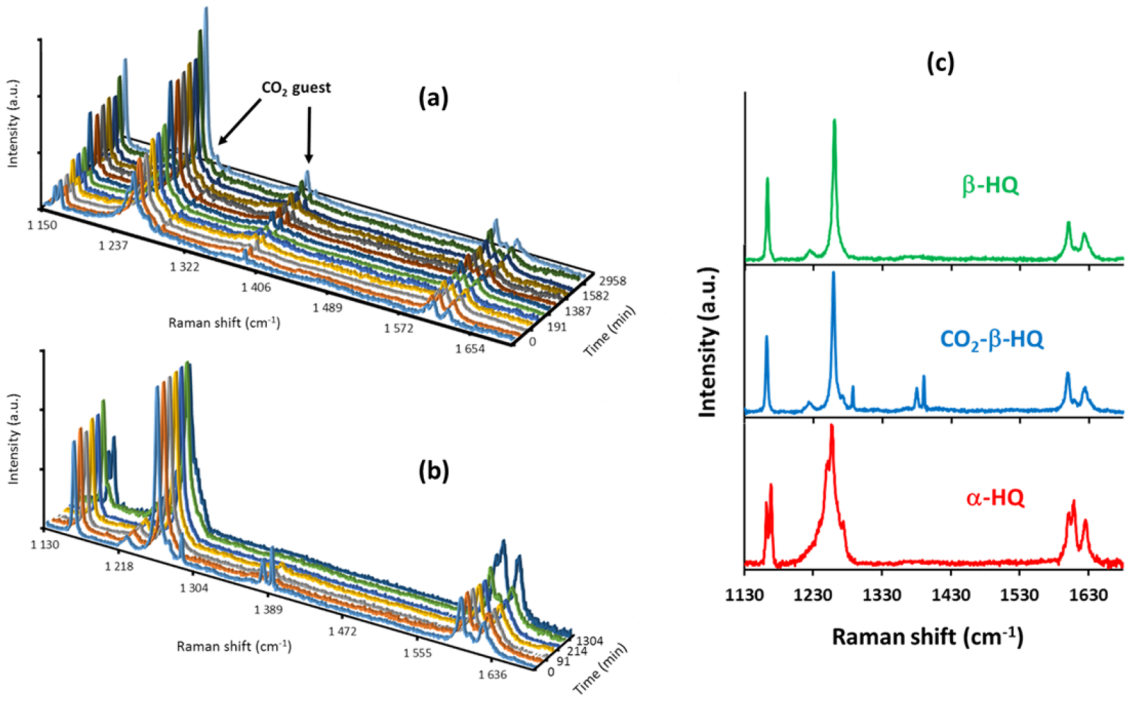

Figure 5. Raman spectroscopic tracking of (a) the formation, at 3.0 MPa and 323 K, and (b) the dissociation, at 1.0 kPa and 343 K, of CO_2–HQ clathrates. (c) Raman spectra of α HQ, CO_2–HQ clathrates, and guest free HQ clathrates. The intensities are given in arbitrary units (a.u.).

"guest molecule release time" (i.e., the time needed for the clathrates to release the guest molecules) was ~3 d.

Formation and Dissociation of the CO_2–HQ Clathrates. Figure 5 presents spectroscopic tracking as a function of the time needed for CO_2–HQ clathrates to form and dissociate.

In the case of CO_2–HQ clathrate formation (Figure 5a), the Raman bands evolved continuously from the spectral signature of α HQ to that of β HQ, and there was also a progressive increase in the intensity of the C═O stretching bands of encaged CO_2 molecules at 1273 and 1380 cm^{-1}. As previously observed, the CO_2 gas bands were also detected at 1287 and 1390 cm^{-1} during the formation step under pressure conditions. At the beginning of the CO_2–HQ clathrate formation phase, we could not detect the guest loaded α HQ intermediate in our experiments, whereas this form does exist and has been already reported in literature data.[3] It can therefore be assumed that the same structural transition process applies for CH_4–HQ clathrate formation and for CO_2–HQ clathrate formation (i.e., a two step reaction passing through the guest loaded α HQ intermediate).

Looking at the spectroscopic tracking of the CO_2–HQ clathrate dissociation (Figure 5b), a gradual decrease in the intensities of the CO_2 band could clearly be seen without there being any changes to those of the β HQ bands, unlike in CH_4–HQ clathrate dissociation. Consequently, once all the CO_2 molecules were released from the host lattice, the spectroscopic signature corresponded unambiguously to that of the guest free HQ clathrates. The Raman spectrum of this intermediate is shown in Figure 5c. The lifetime of this metastable reaction intermediate was an estimated 48 h at most in these dissociation conditions (i.e., 343 K and 1 kPa). After this period the guest free HQ clathrates then gradually returned to a stable α HQ structure. The dissociation of CO_2–HQ clathrates can therefore be described as a two step reaction by eqs 3 and 4:

$$x\mathrm{CO_2}\cdot 3\mathrm{HQ}^{\beta} \rightarrow 3\mathrm{HQ}^{\beta} + x\mathrm{CO_2} \quad (3)$$

$$\mathrm{HQ}^{\beta} \rightarrow \mathrm{HQ}^{\alpha} \quad (4)$$

Concerning the formation and dissociation kinetics of CO_2–HQ clathrates, Figure 6 shows the ratio of the CO_2 band at

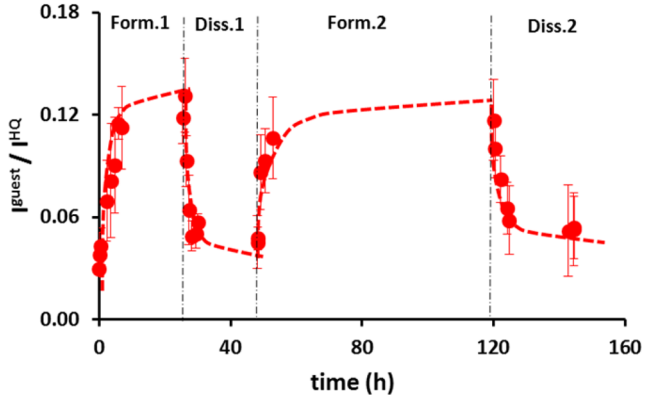

Figure 6. Successive cycles of formation, at 3.0 MPa and 323 K, and dissociation, at 1.0 kPa and 343 K, of CO_2–HQ clathrates. Ratio of intensities of the CO_2 band at 1380 cm^{-1} to the HQ band at 1259 cm^{-1}.

1380 cm^{-1} to the HQ band at 1259 cm^{-1} as a function of time. First of all, we can see that, in the same conditions of pressure and temperature, the formation kinetics of CO_2–HQ clathrates are much faster than those of CH_4–HQ clathrates. Indeed, the induction period was 3.1 ± 0.4 h (instead of 60 ± 10 h for CH_4–HQ clathrate formation), and the release time was ~6 h for CO_2 (instead of 3 d for CH_4). Regarding the clathrate

equilibrium data for CO_2 and CH_4 clathrates only,[26] the proximity of the two equilibrium curves results in a similar distance of the experimental operating point to the equilibrium curves: such a difference in kinetics cannot be explained by thermodynamics, as the difference in driving forces is negligible between the two systems. Accordingly, obviously the formation and the dissociation kinetics of these clathrates are highly dependent on the intrinsic nature of the guest molecules.

In addition, to check the recycling effect of the reactive medium (i.e., the possibility to reuse the α HQ after the clathrate dissociation), two successive reaction cycles (a formation step followed by a regeneration step) were performed using HQ and CO_2 in the same pressure and temperature conditions as discussed previously (i.e., formation at 3.0 MPa and 323 K and dissociation at 1.0 kPa and 343 K). In the two cycles, we observed: (i) the direct formation of CO_2−HQ clathrates from α HQ, and (ii) the dissociation of the CO_2−HQ clathrates to α HQ via the guest free HQ clathrates. As observed in Figure 6, both the formation and dissociation kinetics in the second run were improved (i.e., the reaction time to reach the equilibrium plateau during the second run was ∼2 h faster compared to the first run, shortening the reaction time by ∼30%). Moreover, we measured a decrease in the induction period, which dropped to 0.6 ± 0.2 h (instead of 3.1 ± 0.4 h for the first formation run). These improvements can be attributed to a phenomenon of "HQ structuration" occurring during the first formation/dissociation cycle. With the help of the camera (used to focus the laser on the crystals), we noticed that the crystals after the first cycle presented a rough aspect with distinguishable surface asperities, unlike native HQ crystals, which have smooth, regular surfaces. These modifications in the morphology of the crystals seemingly increased the contact surface area between the HQ and the CO_2 (compared to the native crystals), and as a result created new "nucleation" sites conducive to faster crystallization during the second formation phase. Unfortunately, the camera mounted on the Raman apparatus was unsuitable for recording or taking snapshots to support the above descriptions. Similar observations on CO_2−HQ clathrate monocrystals have already been reported, however (including detailed comparisons with α HQ crystals).[29] This "pre forming effect" of HQ, occurring during the first formation dissociation cycle, opens an interesting avenue of research for enhancing enclathration kinetics.

Global Mechanism. With reference to the previous sections, it is possible to determine general trends as regards HQ clathrate formation and dissociation mechanisms. Indeed, because of the rapid formation of CO_2−HQ clathrates (compared to CH_4−HQ clathrates), we can assume that the CO_2 α HQ intermediate had already formed but went undetected during our experiments. Similarly, the very slow release of CH_4 molecules during the CH_4−HQ clathrate dissociation (compared to the faster dissociation of CO_2−HQ clathrates) might have prevented the detection of guest free HQ clathrates, as the α/β reversion time is roughly the same as the guest molecule release time. These observations would suggest that the lifetimes of the intermediates (i.e., guest loaded α HQ and guest free β HQ) are directly related to the HQ clathrate formation or dissociation kinetics. It is important to note that kinetics are particularly influenced by the pressure and temperature conditions: the induction period is reduced at high pressure,[14] and the enclathration kinetics are faster at high temperature.[23] For this reason, our experimental conditions might not be suitable for observing the CO_2 α HQ intermediate during CO_2−HQ clathrate formation and the guest free clathrates during CH_4−HQ clathrate dissociation. Although we failed to detect or observe the intermediate guest loaded α HQ of CO_2 and the intermediate guest free β HQ of CH_4, extensive experimental evidence has been reported in literature indicating that (i) the guest loaded α HQ intermediate can be obtained with several guest molecules (e.g., CO_2, SO_2, Ar, N_2, and H_2),[2,3,6−10] and (ii) the guest free β HQ can be obtained by heating HQ clathrates formed with guests with different chemical properties (e.g., CO_2 and Xe).[19−21] In the light of all our observations, on the basis of two clathrate systems that form and dissociate with very different kinetics, we could propose the following global mechanism for HQ clathrate formation (eqs 5 and 6) and dissociation (eqs 7 and 8):

$$18HQ^{\alpha} + x^{\alpha}G \rightarrow x^{\alpha}G{\cdot}18HQ^{\alpha} \quad (5)$$

$$x^{\alpha}G{\cdot}18HQ^{\alpha} + (6x - x^{\alpha})G \rightarrow 6[xG{\cdot}3HQ^{\beta}] \quad (6)$$

$$xG{\cdot}3HQ^{\beta} \rightarrow 3HQ^{\beta} + xG \quad (7)$$

$$HQ^{\beta} \rightarrow HQ^{\alpha} \quad (8)$$

where G is a guest molecule.

Selective Gas Capture by HQ Clathrate Formation. The results presented in this section concern the equimolar CO_2/CH_4 gas mixture. Following our previous conclusion that the kinetics are improved after the first formation−dissociation run, these experiments were conducted using the products obtained after CH_4− and CO_2−HQ clathrate dissociation (i.e., either regenerated α HQ or guest free β HQ clathrates). The latter were put in contact with the CO_2/CH_4 gas mixture within 24 h after they had formed. Figure 7 presents the evolution over time of the intensity ratio of the guest band (i.e., CO_2 band at 1380 cm^{-1} and CH_4 band at 2904 cm^{-1}) to the HQ band at 1259 cm^{-1}, and Figure 8 shows the intensity ratio of the CO_2 band to the CH_4 band (referred to as I^{CO2}/I^{CH4} in the following) over time.

First of all, looking at the Raman spectra of the equimolar CO_2/CH_4 gas mixture (presented previously in Figure 2c), we could see that the band intensity of the C−H stretching mode characteristic of CH_4 molecules was stronger than the band intensity of the C═O stretching mode characteristic of CO_2 molecules. Indeed, the intensity ratio of the CO_2 band at 1390 cm^{-1} to the CH_4 band at 2915 cm^{-1} is ∼0.2. Moreover, Zhou et al. proved experimentally that the intensity of the CO_2 band is lower than that of CH_4 for mixed CO_2/CH_4 clathrate hydrates in which the proportion of CO_2 and CH_4 is the same.[35] Therefore, this observation implies that the response factor of CO_2 is lower than that of CH_4 even when the gas molecules retained in clathrate lattices are spatially constrained (i.e., entrapped in a solid phase). Consequently, in our experiments involving the formation of mixed CO_2/CH_4 HQ clathrates, it should be logical that the intensity of the CO_2 band at 1380 cm^{-1} be lower than that of CH_4 at 2904 cm^{-1} (i.e., $I^{CO2}/I^{CH4} < 1$). If the intensity of the CO_2 band was found to be equal to or higher than that of CH_4 (i.e., $I^{CO2}/I^{CH4} \geq 1$), this would mean that there is a significant capture selectivity toward CO_2 molecules.

First, the regenerated α HQ from the CH_4−HQ clathrate dissociation (noted α HQ^{CH4}) was put in contact with the CO_2/CH_4 gas mixture. As shown in Figures 7a and 8, when the

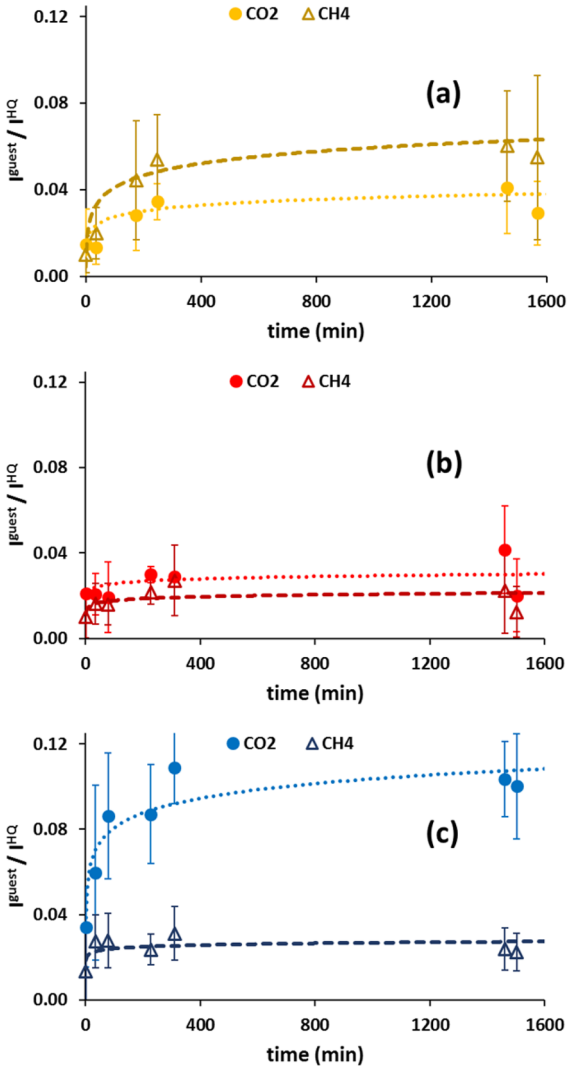

Figure 7. Reaction between the equimolar CO_2/CH_4 mixture and the regenerated α HQ resulting from (a) CH_4– or (b) CO_2–HQ clathrate dissociation, or (c) the guest free β HQ at 3.0 MPa and 323 K. Ratio of intensities of the guest band to the HQ band at 1259 cm^{-1}: (●) CO_2 band at 1380 cm^{-1} and (Δ) CH_4 band at 2904 cm^{-1}.

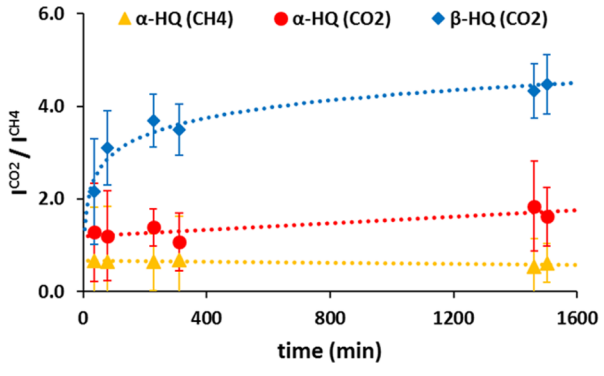

Figure 8. Reaction between the equimolar CO_2/CH_4 mixture and the regenerated α HQ resulting from (▲) CH_4– or (●) CO_2–HQ clathrate dissociation, or (♦) the guest free β HQ at 3.0 MPa and 323 K. Ratio of intensities of the CO_2 band at 1380 cm^{-1} to the CH_4 band at 2904 cm^{-1}.

CO_2/CH_4 gas mixture came into contact with the α HQ^{CH4}, the intensities of both the CO_2 and CH_4 guest bands increased after a reaction time of 1 d. At this point, the intensity of the CO_2 band was observed to be 0.7 times lower than that of the CH_4. However, as we did not know the I^{CO2}/I^{CH4} threshold value at which the amount of CO_2 in the solid started to exceed that of CH_4, we could not come to any conclusion as regards the selective behavior of the α HQ^{CH4} toward CO_2 or CH_4. However, we were able to deduce an induction period of 14.3 ± 10.1 h. Interestingly enough, this induction period fell between those found for pure CO_2–HQ and pure CH_4–HQ clathrates (i.e., 3.1 ± 0.4 h and 60.1 ± 10.0 h for CO_2– and CH_4–HQ clathrates, respectively).

Similarly, when the same gas mixture came into contact with the α HQ obtained from the CO_2–HQ clathrate dissociation (noted α HQ^{CO2}), both the CO_2 and CH_4 band intensities increased after a reaction time of 1 d (see Figures 7b and 8). In this case, the induction period was an estimated 14.8 ± 9.6 h, a value very close to the previous one determined for the α HQ^{CH4} (i.e., 14.3 ± 10.1 h). So, it seems that the induction period when starting with regenerated α HQ does not depend on the guest used for the preforming step. However, the intensity of the CO_2 band was observed to be 1.5 times higher than that of the CH_4 band (i.e., $I^{CO2}/I^{CH4} > 1$) suggesting more CO_2 molecules than CH_4 molecules trapped in the clathrates. This observation implies that the clathrates formed in these conditions contain more CO_2 than CH_4, which proves that the enclathration reaction is selective toward CO_2. It is impossible to precisely determine the exact value of this selectivity (i.e., the molar ratio between the quantity of CO_2 and CH_4 trapped in the clathrate), as this type of quantitative analysis cannot be completed using Raman spectroscopy.

Finally, when the CO_2/CH_4 gas mixture came into contact with the guest free HQ clathrates (as shown in Figures 7c and 8), we observed a dramatic increase in the intensity of the CO_2 band compared to that of the CH_4 one. As the band corresponding to the encaged CO_2 appeared once the Raman cell was pressurized with the gas mixture, it could be concluded that no induction period was required in that case. The intensity ratio for this CO_2 band was observed to be 5 times greater than that for CH_4 (i.e., $I^{CO2}/I^{CH4} \gg 1$). This observation suggests that the guest free HQ clathrates selectively capture a large number of CO_2 molecules from the CO_2/CH_4 gas mixture. This observation had already been suggested in literature[19] but without any direct comparison between the selective behavior of the α HQ and that of the guest free clathrates. We could therefore conclude that both the regenerated α HQ^{CO2} and guest free HQ clathrates preferen tially captured the CO_2 molecules contained in the equimolar CO_2/CH_4 gas mixture. However, the guest free HQ clathrates were able to capture the CO_2 in a much more efficient manner (higher selectivity and faster kinetics) than the α HQ^{CO2}. It is worth noting that the selective performance of the enclathra tion reaction starting with α HQ^{CO2} and from a guest free structure derived from CO_2 clathrates had never been compared before. In literature, authors who had also come across this type of selective enclathration succinctly explained the phenomenon by a dynamical aperture widening process of the guest free HQ clathrate cavities, whose access diameter is ~3 Å.[19] However, we believe that such an "aperture widening process" is not specific to CO_2 molecules. According to the results obtained for the reactions between the equimolar CO_2/CH_4 gas mixture and either the α HQ^{CH4}, α HQ^{CO2}, or guest free β HQ, it can be inferred that three main factors related to guest molecules are likely to impact the capture selectivity: (i)

molecular sizes, (ii) kinetic diameters, and (iii) the electrostatic nature of the guests involved. The two experiments performed with α HQ^{CH4} and α HQ^{CO2} indicated that the preforming steps with CH_4 or CO_2 led to the creation of materials that exhibited greater selectivity toward the gas used to preform the structure. In this case, the cavities in the regenerated α HQ would be specific to the guest due to steric hindrance, as the molecular sizes of CH_4 and CO_2 are 4.36 and 5.12 Å, respectively.[36] This conclusion also applies to the guest free β HQ obtained from the CO_2−HQ clathrate dissociation (i.e., the guest free β HQ cavities could essentially be compatible with the size of CO_2 molecules). As suggested by McAdie,[37] a cavity once sufficiently distorted to allow the guest to be released would remain so, allowing re entry by a "truly reversible" process. Moreover, the kinetic diameter of CH_4 (3.8 Å) is higher than that of CO_2 (3.3 Å),[38] suggesting that CO_2 can permeate more easily through the guest free β HQ (by analogy with molecular sieving, where the separation efficiency depends on the kinetic diameters of the species). Additionally, because of its electrostatic nature, the CO_2 guest molecule could be attracted into the clathrate cavities due to the partial charge in the atoms, as proposed in literature.[23] Given the position of CO_2 molecules in HQ clathrate cavities (all aligned toward the c axis of the structure),[29] the positively charged carbon atoms of CO_2 are located at the center of the cavities, and the negatively charged oxygen atoms at the top and the bottom of the cavity.[39] These different points (i.e., the difference in molecular size, kinetic diameter, and electrostatic nature between CH_4 and CO_2) could also explain the differences in the formation and dissociation kinetics observed for the CH_4− and CO_2−HQ clathrates. Finally, one of the main conclusions to keep in mind concerning the selective process of gas capture by HQ clathrates is that higher CO_2 selectivity is obtained when the CO_2/CH_4 gas mixture is in direct contact with the guest free clathrates derived from the CO_2−HQ clathrates.

■ CONCLUSIONS

This study was devoted to understanding the formation and dissociation mechanisms of HQ clathrates, as well as providing additional results in terms of kinetics and innovative elements in an attempt to explain why, in some cases, HQ clathrates exhibit high selectivity toward CO_2. A CO_2/CH_4 gas mixture was chosen, because the separation of CO_2 from this mixture is a very important case study for practical applications frequently encountered in the oil and gas industry. The results presented were obtained by means of Raman spectroscopy, an ideal analytical technique for tracking the kinetics and structural evolutions of these compounds, forming a transient metastable phase, in situ over time. The experiments were performed using a customized Raman cell, which enabled us to track the spectroscopic signatures of the samples under pressure and temperature conditions set at 323 K and 3.0 MPa for the clathrate formation stage and at 343 K and 1.0 kPa for the dissociation step. On the one hand, by performing experiments on CH_4−HQ clathrates (which form and dissociate relatively slowly), we found that gas molecules were first trapped in the cavities of the α HQ by "solubilization in the α phase" thus creating the CH_4 α HQ intermediate before formation of the clathrates. On the other hand, experiments conducted with CO_2−HQ clathrates (which form and dissociate much quicker than CH_4−HQ clathrates) confirmed the presence of the guest free HQ clathrate intermediate before the HQ clathrates returned to their native α form. On the basis of these combined observations, a global mechanism could be proposed: α HQ in the presence of the right guest molecule and in appropriate thermodynamic conditions forms HQ clathrates, passing through the stage of guest loaded α HQ intermediates; if the thermodynamic conditions are then suitable for clathrate dissociation, the HQ clathrates return to their native form passing through a metastable guest free structure. It is worth noting that the detection of these intermediates seems to be highly dependent on the experimental conditions. Moreover, in the same conditions of temperature and pressure, it was clearly demonstrated that (i) the formation and the dissociation kinetics of the CO_2−HQ clathrates are faster than those of the CH_4−HQ clathrates, and (ii) the difference in kinetics is guest dependent and not related to thermodynamics, as the CH_4− and CO_2−HQ clathrate equilibrium curves are very close to each other. Experiments involving several formation/dissociation cycles on the same HQ sample also revealed that HQ could be reused after the first cycle and that this "pre forming step" enhanced both the clathrate formation and dissociation kinetics for the following cycles. Finally, both the α HQ and the guest free HQ clathrates obtained from the CO_2−HQ clathrate dissociation preferentially capture the CO_2 contained in an equimolar CO_2/CH_4 gas mixture. The higher capture selectivity toward CO_2 was only obtained by putting the gas mixture in contact with the guest free HQ clathrate intermediate derived from the CO_2 clathrates. This last point shows that, although HQ are selective toward CO_2 at the pressure and temperature conditions of this study, the key to capturing CO_2 more selectively and efficiently is to perform the enclathration reaction using the guest free intermediate derived from the CO_2−HQ clathrates.

■ AUTHOR INFORMATION

Corresponding Author

*Phone: +335 40 17 51 09. E mail: jean philippe.torre@univ pau.fr.

ORCID

Christophe Dicharry: 0000 0002 6318 3989

Jean-Philippe Torré: 0000 0001 5735 8626

Author Contributions

All authors contributed extensively to the work presented in this paper and have approved the final version.

Notes

The authors declare no competing financial interest.

■ ACKNOWLEDGMENTS

We would like to acknowledge the entire work group involved in the ORCHIDS project and the ISIFoR Carnot Institute (Institute for the Sustainable engIneering of Fossil Resources). The authors would also like to thank the Gas Solutions department of Total S.A. (E&P Division) for its financial support. We extend our warmest thanks to J. Diaz and J. P. Grenet for their technical assistance with the apparatus.

■ ABBREVIATIONS

HQ, hydroquinone

■ REFERENCES

(1) Mak, T. C. W.; Lam, C. K. *Encyclopedia of Supramolecular Chemistry;* Atwood, J. L., Steed, J. W., Eds.; CRC Press, Taylor & Francis Group: Boca Raton, FL, 2004; Vol. *1*, pp 679−686.

(2) Wallwork, S. C.; Powell, H. M. The Crystal Structure of the α Form of Quinol. *J. Chem. Soc., Perkin Trans. 2* **1980**, *2*, 641−646.
(3) Powell, H. M. The Structure of Molecular Compounds. Part IV. Clathrate Compounds. *J. Chem. Soc.* **1948**, 61−73.
(4) Maartmann Moe, K. The Crystal Structure of γ Hydroquinone. *Acta Crystallogr.* **1966**, *21*, 979.
(5) Naoki, M.; Yoshizawa, T.; Fukushima, N.; Ogiso, M.; Yoshino, M. A New Phase of Hydroquinone and its Thermodynamic Properties. *J. Phys. Chem. B* **1999**, *103*, 6309−6313.
(6) Yoon, J. H.; Lee, Y. J.; Park, J.; Kawamura, T.; Yamamoto, Y.; Komai, T.; Takeya, S.; Han, S. S.; Lee, J. W.; Lee, Y. J. Hydrogen Molecules Trapped in Interstitial Host Channels of α Hydroquinone. *ChemPhysChem* **2009**, *10*, 352−35.
(7) Powell, H. M. The Structure of Molecular Compounds. Part VII. Compounds Formed by the Inert Gases. *J. Chem. Soc.* **1950**, 298−300.
(8) Chekhova, G. N.; Polyanskaya, T. M.; Dyadin, Y. A.; Alekseev, V. I. Clathrates of Hydroquinone. II. Chemical and X ray Phase Analysis of the Solid Phases in the Hydroquinone Water Sulfur Dioxide System. *J. Struct. Chem.* **1976**, *16*, 966−971.
(9) Marsh, R. E. The Space Groups of Point Group C3: Some Corrections, Some Comments. *Acta Crystallogr., Sect. B: Struct. Sci.* **2002**, *58*, 893−899.
(10) Polyanskaya, T. M.; Andrianov, V. I.; Alexeev, V. I.; Bakakin, V. V.; Dyadin, Y. A.; Chekhova, G. N. Clathrate Crystal Structure of α Hydroquinone with Sulfur Dioxide. *Soviet Physics Doklady* **1982**, *27*, 684.
(11) Coupan, R.; Plantier, F.; Torré, J. P.; Dicharry, C.; Sénéchal, P.; Guerton, F.; Moonen, P.; Khoukh, A.; Kessas, S. A.; Hemati, M. Creating Innovative Composite Materials to Enhance the Kinetics of CO_2 Capture by Hydroquinone Clathrates. *Chem. Eng. J.* **2017**, *325*, 35−48.
(12) Conde, M. M.; Torré, J. P.; Miqueu, C. Revisiting the Thermodynamic Modelling of Type I Gas Hydroquinone Clathrates. *Phys. Chem. Chem. Phys.* **2016**, *18*, 10018−10027.
(13) Helle, J. N.; Kok, D.; Platteeuw, J. C.; Van der Waals, J. H. Thermodynamic Properties of Quinol Clathrates III. *Recl. Trav. Chim.* **1962**, *81*, 1068−1074.
(14) Allison, S. A.; Barrer, R. M. Clathration by Phenol and Quinol. Part. II Kinetics. *Trans. Faraday Soc.* **1968**, *64*, 557−565.
(15) Steed, J. W.; Turner, D. R.; Wallace, K. J. *Core Concepts in Supramolecular Chemistry and Nanochemistry;* John Wiley & Sons: Chichester, England, 2007; pp 179−194.
(16) Rozsa, V. F.; Strobel, T. A. Triple Guest Occupancy and Negative Compressibility in Hydrogen Loaded β Hydroquinone Clathrate. *J. Phys. Chem. Lett.* **2014**, *5*, 1880−1884.
(17) Evans, D. F.; Richards, R. E. Preparation and Magnetic Susceptibility of an Oxygen Clathrate Compound. *Nature* **1952**, *170*, 246.
(18) Clausen, H. F.; Chen, Y. S.; Jayatilaka, D.; Overgaard, J.; Koutsantonis, G. A.; Spackman, M. A.; Iversen, B. B. Intermolecular Interactions and Electrostatic Properties of the β Hydroquinone Apohost: Implications for Supramolecular Chemistry. *J. Phys. Chem. A* **2011**, *115*, 12962−12972.
(19) Lee, Y. J.; Han, K. W.; Jang, J. S.; Jeon, T. I.; Park, J.; Kawamura, T.; Yamamoto, Y.; Sugahara, T.; Vogt, T.; Lee, J. W.; et al. Selective CO_2 Trapping in Guest free Hydroquinone Clathrate Prepared by Gas Phase Synthesis. *ChemPhysChem* **2011**, *12*, 1056−1059.
(20) Han, K. W.; Lee, Y. J.; Jang, J. S.; Jeon, T. I.; Park, J.; Kawamura, T.; Yamamoto, Y.; Sugahara, T.; Vogt, T.; Lee, J. W.; et al. Fast and Reversible Hydrogen Storage in Channel cages of Hydroquinone Clathrate. *Chem. Phys. Lett.* **2012**, *546*, 120−124.
(21) Ilczyszyn, M.; Selent, M.; Ilczyszyn, M. M. Participation of Xenon Guest in Hydrogen Bond Network of β Hydroquinone Crystal. *J. Phys. Chem. A* **2012**, *116*, 3206−3214.
(22) Falenty, A.; Hansen, T. C.; Kuhs, W. F. Formation and Properties of Ice XVI Obtained by Emptying a Type sII Clathrate Hydrate. *Nature* **2014**, *516*, 231−233.
(23) Lee, J. W.; Yoon, J. H. Preferential Occupation of CO_2 Molecules in Hydroquinone Clathrates Formed from CO_2/N_2 Gas Mixtures. *J. Phys. Chem. C* **2011**, *115*, 22647−22651.
(24) Lee, J. W.; Dotel, P.; Park, J.; Yoon, J. H. Separation of CO_2 from Flue Gases Using Hydroquinone Clathrate Compounds. *Korean J. Chem. Eng.* **2015**, *32*, 2507−2511.
(25) Lee, J. W.; Poudel, J.; Cha, M.; Yoon, S. J.; Yoon, J. H. Highly Selective CO_2 Extraction from a Mixture of CO_2 and H_2 Gases Using Hydroquinone Clathrates. *Energy Fuels* **2016**, *30*, 7604−7609.
(26) Coupan, R.; Chabod, M.; Dicharry, C.; Diaz, J.; Miqueu, C.; Torré, J. P. Experimental Determination of Phase Equilibria and Occupancies for CO_2, CH_4, and N_2 Hydroquinone Clathrates. *J. Chem. Eng. Data* **2016**, *61*, 2565−2572.
(27) Kubinyi, M. J.; Keresztury, G. Infrared and Raman Spectra of Hydroquinone Crystalline Modifications. *Mikrochim. Acta* **1997**, *14*, 525−528.
(28) Jakobsen, R. J.; Brewer, E. J. Vibrational Spectra of Benzene Derivatives. I. Para Substituted Phenols. *Appl. Spectrosc.* **1962**, *16*, 32−35.
(29) Torré, J. P.; Coupan, R.; Chabod, M.; Péré, E.; Labat, S.; Khoukh, A.; Brown, R.; Sotiropoulos, J. M.; Gornitzka, H. CO_2 Hydroquinone Clathrate: Synthesis, Purification, Characterization and Crystal Structure. *Cryst. Growth Des.* **2016**, *16*, 5330−5338.
(30) Park, J. W.; An, S.; Seo, Y.; Kim, B. S.; Yoon, J. H. Temperature Dependent Release of Guest Molecules and Structural Transformation of Hydroquinone Clathrates. *J. Phys. Chem. C* **2013**, *117*, 7623−7627.
(31) Kohl, A.; Nielsen, R. *Gas Purification;* Gulf Publishing Company: Houston, TX, 1997.
(32) Lee, J. W.; Choi, K. J.; Lee, Y.; Yoon, J. H. Spectroscopic Identification and Conversion Rate of Gaseous Guest loaded Hydro quinone Clathrates. *Chem. Phys. Lett.* **2012**, *528*, 34−38.
(33) Davies, J. E. D. Clathrates and Inclusion Compounds. Part I. Infrared and Raman Studies of Several β Quinol (Hydroquinone) Clathrates. *J. Chem. Soc., Dalton Trans.* **1972**, *11*, 1182−1188.
(34) Lee, J. W.; Lee, Y.; Takeya, S.; Kawamura, T.; Yamamoto, Y.; Lee, Y. J.; Yoon, J. H. Gas Phase Synthesis and Characterization of CH_4 Loaded Hydroquinone Clathrates. *J. Phys. Chem. B* **2010**, *114*, 3254−3258.
(35) Zhou, X.; Long, Z.; Liang, S.; He, Y.; Yi, L.; Li, D.; Liang, D. In Situ Raman Analysis on the Dissociation Behavior of Mixed CH_4−CO_2 Hydrates. *Energy Fuels* **2016**, *30*, 1279−1286.
(36) Sloan, E. D.; Koh, C. A. *Clathrate Hydrates of Natural Gases,* 3rd ed.; CRC Press, Taylor & Francis Group: Boca Raton, FL, 2008.
(37) McAdie, H. G. Thermal Decomposition of Molecular Complexes: II. β Quinol Clathrates. *Can. J. Chem.* **1963**, *41*, 2137−2143.
(38) Ismail, A. F.; Khulbe, K. C.; Matsuura, T. *Gas Separation Membranes, Polymeric and Inorganic;* Springer International Publishing: Switzerland, 2015.
(39) Zubkus, V. E.; Shamovsky, I. L. Molecular Interactions, Structure and Stability of β Quinol Clathrate. *Chem. Phys. Lett.* **1992**, *195*, 135−143.